Orientational Order and Dynamics of Nematic Multipodes Based on Carbosilazane Cores Using Optical and Dielectric Spectroscopy

L. Tajber,[†] A. Kocot,[‡] J. K. Vij,*[,†] K. Merkel,[†] and J. Zalewska-Rejdak[†]

Laboratory of Advanced Materials, Department of Electronic Engineering, Trinity College, University of Dublin, Dublin 2, Ireland, and Institute of Physics, University of Silesia, Katowice, Poland

G. H. Mehl,[§] R. Elsässer,[§] J. W. Goodby,[§] and M. Veith[⊥]

Department of Chemistry, University of Hull, Cottingham Road, Hull HU6 7RX, United Kingdom, and University of Saarland, Saarbrücken, Germany

Received May 9, 2002; Revised Manuscript Received August 5, 2002

ABSTRACT: The birefringence, refractive indices, and dielectric measurements have been carried out for the double- and triple-branched multipodes based on the carbosilazane cores. The orientational order parameters have been obtained using both the optical and the dielectric measurements. The dielectric response is identified to arise from the dipoles of the carboxyl and the alkoxy groups in the ortho position of the benzene ring. Results are analyzed in the framework of the mean-field theory. At least three molecular modes are resolved in the dielectric relaxation spectra in the nematic phase. The lower frequency process is retarded, and the other two processes are accelerated significantly with respect to the relaxation rate in the isotropic phase. The acceleration effect is even much stronger than the retardation effect. The acceleration factors are also found to be much higher than those for the low molar mass nematic liquid crystals. These results show that the anisotropy of the macromolecule plays a significant role in determining the nematic potential which governs the relaxation dynamics. The results on the relaxation dynamics show that the mesogens are decoupled from the core of the macromolecules.

1. Introduction

Macromolecular architecture has received considerable and increasing interest during the recent years. Dendrimers and structurally related multipodes represent a class of macromolecules with a perfectly branched uniform structure,[1,2] in contrast to hyperbranched polymers where the branching occurs in a random fashion. Dendrimers are synthesized through a stepwise, repetitive reaction sequence that guarantees complete shells for each generation, leading to polymers that are monodispersive. The synthetic procedures permit nearly complete control over the critical molecular design parameters, such as the shape, size, viscosity, flexibility, and topology.[3,4]

Investigations on multipodal and dendritic liquid crystal systems have so far mainly been focused on the materials that perform layered, columnar, and cubic-phase structures.[5] However, the systems that exhibit nematic phase behavior have also recently attracted considerable attention. Such a system is controlled only by the orientational ordering, and the functional groups promote nanoscopic phase or nanophase separation. The structural concept allows the docoupling of the mesomorphic behavior and the ordering of the LC phase from the size of the molecules. This leads to the macromolecules with LC properties similar to those of comparable low molar mass liquid crystals.

2. Experimental Section

2.1. Description of the Compound. Carbosilazane cores, which display an overall 3-fold symmetry, have been used for obtaining microphase-separated systems, as reported earlier.[6−8] The desired nematic phase behavior was achieved by using the mesogenic group A, whose synthesis has been reported previously.[8] The mesogen core consists of three aromatic rings connected by an ester group (with ester group linkage). The core was flanked by terminal octyl and undecyl groups linked to the dendritic core through a short lateral spacer of five methylene groups and a 1,1,3,3-tetramethyldisiloxane group (Figure 1). The structure was judged to give the appropriate balance between the coupling and the flexibility and thus found suitable for achieving the nematic phase and for avoiding the appearance of the higher ordered liquid crystalline phases.

All synthesized products of this series show enantiotropic nematic phase behavior. Polarized light microscopy of these compounds shows typical nematic textures of low viscosity (schlieren texture) with two and four brush defects on cooling from the isotropic to the liquid crystalline state. The transition temperatures and the associated enthalpies and entropies have been established for the second heating cycles using differential scanning calorymetry (DSC)[8] (see Table 1 in ref 8). The relatively low values for the transition enthalpies (ΔH) ranging from 0.31 to 0.7 J g^{-1} of this series as compared to those of other nematic systems suggest the presence of a low ordered system. Normalized isotropization entropy $(\Delta S/R)n^{-1}$ which is related to the nematic ordering at the isotropization temperature is found almost independent of the size of molecule whether it is low molar mass material or dendritic polymer. The results for transition temperatures, enthalpies, and normalized isotropization entropy indicate that these dendrimers exhibit very similar LC properties that are not very different from those of comparable low molar mass compounds.

2.2. Refractive Index and Birefringence Measurements. Refractive indices of liquid crystals may be measured by a variety of methods, but all of these methods require a well-aligned thin film. We use a simple method of Abbe refractometer (Bellingham&Stanley Ltd., model 60/ED) with a suitably coated prism surface and use a polarizer, which permits the separation of the two refracted rays. Homeotropic

[†] Trinity College.
[‡] University of Silesia.
[§] University of Hull.
[⊥] University of Saarland.
* Corresponding author: e-mail jvij@tcd.ie.

10.1021/ma020714p CCC: $22.00
Published on Web 09/28/2002

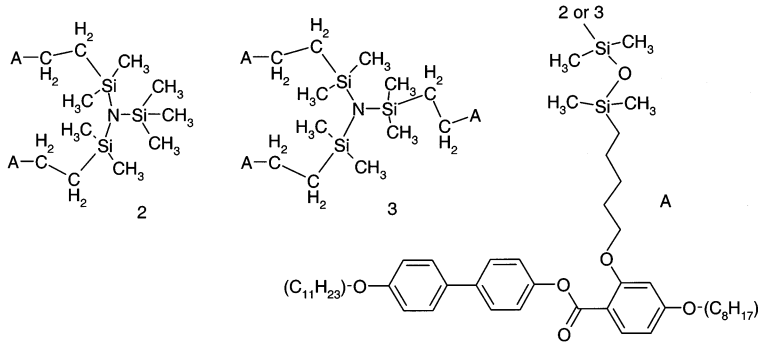

2A: Cr -12.6° C N 37.5° C Iso

3A: T_g -26.0° C N 41.6° C Iso

Figure 1. Structure of the dendrimers. Multipodal cores for **2A** and **3A** dendrimers are labeled as 2 and 3; the mesogen is labeled as A.

alignment on prisms surfaces was achieved by using 0.5% solution of lecithin in chloroform. The LC was placed between the prisms with sufficient amount (approximately 0.5 mL) that it fills the gap between them when closed. After the filling of the system so described, it was left for some time (2−3 h) for the best alignment to develop. Positions of the boundaries that we observe correspond to the values of $n_e = n_{||}$ and $n_0 = n_\perp$. These values of indices were read from scale using a polarizer mounted outside on the eyepiece to look at the polarization of the output light. The boundaries viewed in the instrument are orthogonally polarized for each of the refractive indices. This Abbe refractometer has prisms that allow measurements of the refractive index of substances between 1.300 and 1.700. A monochromatic sodium lamp (wavelength 589.6 nm) as a source of light was used. Temperature was controlled with an accuracy of ±0.05 K.

Birefringence measurements were performed using a homemade LC cell. Glass plates with ITO layers were spin-coated with PVA solution (0.3% poly(vinyl alcohol) solution) and then baked for 1 h at 125 °C to remove the solvent residue and polymerize the aligning medium. Glasses were rubbed unidirectionally on velvet track in order to achieve a homogeneous planar orientation. The LC dendrimer was introduced into the cell by capillary action in the isotropic phase (a few degrees above the phase transition temperature). The cell thickness calculated from the measured capacitance of the empty cell was $d = 7.16$ μm.

The optical properties of dendrimers **2A** and **3A** are investigated in the nematic phase by polarizing microscope POLAM P-312 ("Lomo", St. Petersburg, Russia) with Tilting Compensator (Leitz, Germany). During measurements, different filters of wavelengths blue 494 nm, white 546 nm, yellow 587 nm, and red 619 nm were used.

Both refractive indices and birefringence results show great accuracy and accordingly also determine the isotropic-to-nematic phase transition. However, the results of Δn are found to be lower from the Abbe refractometer than determined using the tilting compensator method. This was presumably due to the reason that perfect homeotropic alignment in the former method was not reached. Finally, we took results of Δn obtained by the tilting compensator method (as these are much more accurate and are made on the well-defined homogeneous alignment). The Abbe refractometer results are used for finding the mean refractive index n, where $n^2 = (2n_0^2 + n_e^2)/3$ (Figure 2). In this figure, $n_e = n_{||}$ and $n_0 = n_\perp$.

2.3. Dielectric Measurements. Sample cells for dielectric measurements were prepared using gold-plated brass electrodes. For planar alignment, the conducting inner surfaces were spin-coated with 0.3% poly(vinyl alcohol), PVA, alignment layer and rubbed unidirectionally. The cell thickness was $d \cong 15$ μm. Cells were filled in the nematic phase at about 5 K below the isotropization temperature.

The dielectric permittivity ϵ' and loss ϵ'' were measured over the frequency range 0.1 Hz−10 MHz using a broadband dielectric spectrometer (Novocontrol, GMBH, Germany). The temperature in the sample was controlled automatically with the accuracy better than ±0.1 K. The electric voltage applied to the sample was equal to 0.1 V.

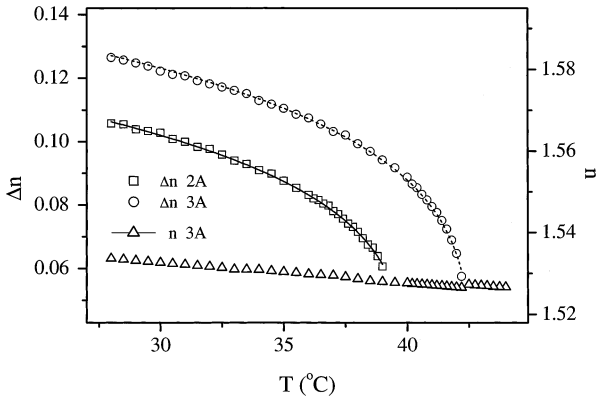

Figure 2. Refractive index $n - \Delta$ and birefringence Δn of **2A** (□) and **3A** (○) dendrimers as a function of temperature.

3. Results and Discussion

3.1. Order Parameter from the Refractive Index and Birefringence Measurements. Most of the applications of liquid crystals are controlled by their optical properties and the response of the liquid crystalline molecules to the electric field and changes in temperature and pressure. The understanding of the relationship between the two refractive indices and the molecular properties is necessary for the design of liquid crystals to tailor the applications. The electronic polarizability is assumed to be independent of temperature,[9] so the temperature dependence of refractive indices is determined primarily by the order parameter and to a lesser extent by changes in the density. Most of the known theories[10,11] on this interrelationship extend the classical Lorenz−Lorentz formula to the ordered fluids, which simply adopts the isotropic model for the internal field and includes the anisotropy of the polarizability.[12]

If we assume the isotropic model for the internal field, the principal refractive indices can be described as

$$\frac{n_i^2 - 1}{n^2 + 2} = \frac{N\langle\alpha_{ii}\rangle}{3\epsilon_0} \qquad (1)$$

where $\langle\alpha_{ii}\rangle$ is the average value of the polarizability,

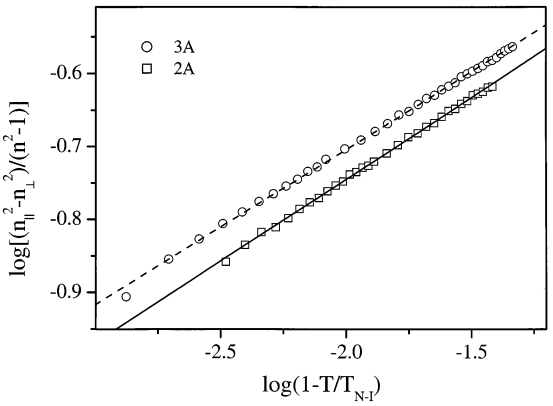

Figure 3. Plot of $\log[(n_{\|}^2 - n_{\perp}^2)/(n^2 - 1)]$ vs $\log(1 - T/T_{N-I})$ for the calculation of anisotropy in the polarizability $\Delta\alpha/\alpha$ of **2A** (□) and **3A** (○) dendrimers. Here T is in K.

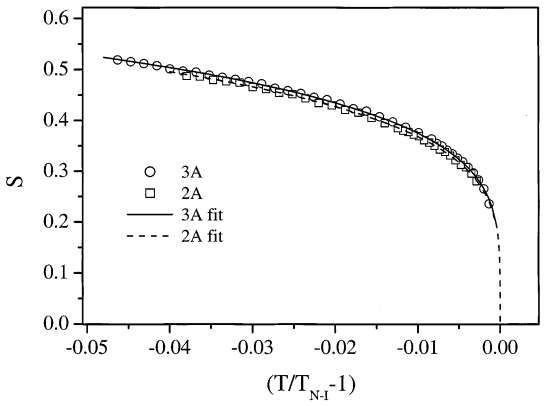

Figure 4. Orientational order parameters calculated from the refractive indices and birefringence data of **2A** (□) and **3A** (○) and fitted to the mean-field theory.

component n_i is the refractive index along the principal axis, and n is the average refractive index. Using the general method for the transformation from molecular to laboratory frame, these polarizabilities can be expressed in terms of the molecular components and the orientational order parameters S and D. Assuming uniaxial symmetry of liquid crystals, the polarizability components parallel and perpendicular[9] to the director are as follow:

$$\langle\alpha_{\|}\rangle = \alpha + \frac{2}{3}\left\{S\left[\alpha_{nn} - \frac{1}{2}(\alpha_{ll} + \alpha_{mm})\right] + \frac{1}{2}D(\alpha_{ll} - \alpha_{mm})\right\}$$

$$\langle\alpha_{\perp}\rangle = \alpha - \frac{1}{3}\left\{S\left[\alpha_{nn} - \frac{1}{2}(\alpha_{ll} + \alpha_{mm})\right] + \frac{1}{2}D(\alpha_{ll} - \alpha_{mm})\right\} \quad (2)$$

where l, m, n are labels for the principal axes of the molecular polarizability.

For most of the nematogens it is reasonable to assume that the molecular shape has axial symmetry ($\alpha_{ll} = \alpha_{mm}$); in that case the contribution from molecular biaxiality, D, can be ignored, and relation 1 is reduced to the form

$$\frac{n_{\|}^2 - n_{\perp}^2}{n^2 - 1} = \frac{S\Delta\alpha}{\alpha} \quad (3)$$

where $\Delta\alpha = \alpha_{nn} - \alpha_{ll}$. It is useful to assume a simple form of the temperature dependence for the order parameter S:

$$S = (1 - T/T_{N-I})^b \quad (4)$$

$\Delta\alpha/\alpha$ can be calculated as an intercept from the linear approximation of a plot of $\log[(n_{\|}^2 - n_{\perp}^2)/(n^2 - 1)]$ vs $\log(1 - T/T_{N-I})$.[9,13]

The linear plots for dendrimers **2A** and **3A** are shown in Figure 3. These are used for the calculation of $\Delta\alpha/\alpha$ from the intercepts of these log−log plots. The polarizability anisotropy, $\Delta\alpha/\alpha$, for dendrimers **2A** and **3A** is found to be 0.505 and 0.527, respectively. These values are very close to the theoretical value for the polarizability anisotropy of 0.55 found for the monomer (see Figure 1, part A) using the Gaussian program (G98W). On using the values of $\Delta\alpha/\alpha$, we can calculate the order parameter, S, from eq 3. The calculated temperature dependence of the order parameters for **2A** and **3A** dendrimers is shown in Figure 4. It is interesting to note that the temperature dependence of S and also the values of $\Delta\alpha/\alpha$ are very similar for both **2A** and **3A** dendrimers, and on the other hand, they are close to the theoretical value obtained from modeling of the monomer structure. These results indicate that nanophase-structured nematic dendrimers show liquid crystalline properties similar to those of the comparable low molar mass compounds.

The critical exponents are found by fitting eq 4 to be 0.22 and 0.225 dendrimers for compounds **2A** and **3A**, respectively. These values are very close to $b = 0.25$, which is typical of the so-called three-critical point of the phase diagram.[14] Such behavior is expected of systems exhibiting with reasonable low values of the transition enthalpies, and the behavior is comparable to other nematic systems. Indeed, the enthalpy has been measured to be as low as $\Delta H = 0.66$ J g^{-1} for both compounds **2A** and **3A**.[8] A detailed analysis of the critical behavior of the order parameter can be carried out using the mean-field (MF) theory of the free energy density expansion:

$$g = \frac{1}{2}A(T - T_{N-I})S^2 + \frac{1}{4}BS^4 + \frac{1}{6}CS^6 + \ldots \quad (5a)$$

In the mean-field approximation, the so-called three-critical behavior corresponds to the case when the second term ($\sim S^4$) in the free energy expansion is close to zero and the next term ($\sim S^6$) is included. The minimization of dg/dS gives the relation for $S(T)$,

$$T_{N-I} - T = \frac{B}{A}S^2 + \frac{C}{A}S^4 \quad (5b)$$

If the term BS^2/A for the three-critical behavior is ignored in (5b), then $S = [A/C(T - T_{N-I})]^{0.25}$. If this is not the case, one can then fit the dependence of S on T using eq 5b. The parameters for the best fit are found to be $B/A = -18.5$ K and $C/A = 240$ K. The fitting is shown later. Since B is found to be negative and much smaller in magnitude than C, the transition is therefore quantified to be a weakly first-order transition.

3.2. Dielectric Measurements. From the dielectric measurements made with the procedure outlined in section 2.3, the dielectric relaxation times are calculated for the homogeneously aligned dendrimers **2A** and **3A** in the nematic and the isotropic phase temperature ranges.

The dielectric spectra are fitted to the Havriliak−Negami equation[15] when extended to n relaxation processes

$$\epsilon^*(\omega) - \epsilon_\infty = \sum_{j=1}^{n} \frac{\Delta\epsilon_j}{(1 + (i\omega\tau_j)^\alpha)^\beta} \quad (6)$$

$\epsilon^*(\omega)$ is the complex permittivity at an angular frequency of ω, ϵ_∞ is the high-frequency permittivity, j denotes the number of relaxation processes from 1 up to n, τ_j is the relaxation time of the jth relaxation process, α and β are the fitting parameters, and $\Delta\epsilon_j$ is dielectric strength for the jth process. The fitting procedure did not require the β parameter to deviate from unity, so β was finally fixed to unity for the entire temperature range of the measurements. In such a case the relaxation time of the particular process is simply related to the angular frequency ω_j or the relaxation frequency f_j as follows: $\tau_j = 1/\omega_j = 1/(2\pi f_j)$. The relaxation frequency is independent of the value of α if $\beta = 1$. For $\beta = 1$, eq 6 reduces to the Cole−Cole equation.

The frequency dependence of the dielectric permittivity can be analyzed for a uniaxial liquid crystal having no local biaxial order. The effect of the induced moment can be easily removed by subtracting the high-frequency part of the permittivity (or square of the refractive index $\epsilon_\infty \cong n^2$).

According to Maier and Meier (M−M) theory,[9,16,17] the perpendicular and parallel components of the real part of the permittivity are related to the orientational order parameter, S, as follows:

$$\epsilon_{||}(\omega) - n_{||}^2 = \frac{NhF^2 g_l^{||}}{3\epsilon_0 k_B T}[\mu_l^2(1 + 2S) + \mu_t^2(1 - S)] \quad (7a)$$

$$\epsilon_{\perp}(\omega) - n_{\perp}^2 = \frac{NhF^2 g_l^{\perp}}{3\epsilon_0 k_B T}\left[\mu_l^2(1 - S) + \mu_t^2\left(1 + \frac{1}{2}S\right)\right] \quad (7b)$$

Each component of $\epsilon(\omega)$ contains two contributions from the molecular dipole moment, and each of these is expected to show three relaxation regions. In general, the dynamics can approximately be described in terms of the three rotational modes:[17] the end-over-end rotation (ω_e), the processional motion (ω_p) about the director, and the rotation (ω_l) about its own long molecular axis, called here the spinning motion. It should be mentioned, however, that ω_p and ω_e are usually not well separated from each other in the frequency spectrum.

3.3. Contribution of the Molecular Modes to the Dielectric Strength. To analyze both perpendicular and parallel components of the dielectric permittivity, samples need to be aligned both homeotropically and homogeneously. However, we do not succeed in achieving a good homeotropic alignment, presumably because of a large size of the molecules. Hence, the results are presented only for the homogeneous alignment (Figure 5). For the homogeneous planar geometry in the nematic phase, it is reasonable to consider the perpendicular $\Delta\epsilon_\perp - \epsilon_{\infty\perp}$ component of the dielectric permittivity. Frequency scans of the real and imaginary components of dielectric permittivity (Figure 5) show three relaxation regions in the dielectric loss, which are centered approximately at frequencies $f_1 = 10^2$ Hz, $f_2 = 10^4$ Hz, and $f_3 = 5 \times 10^5$ Hz. These are also indicated by steps in the real part of permittivity (see Figure 6, not shown in Figure 5). The frequencies of the various modes can be better derived from the peak positions of the permittivity derivative $d\epsilon'/d(\log f)$, as demonstrated in Figure 6. It important to note that high-frequency value of ϵ' ($\epsilon' \cong 12$ at 10^7 Hz) is much greater than the value of ϵ_∞, expected for the high-frequency limit ($\epsilon_\infty \cong n_\perp^2$, $\epsilon_\infty \cong 2.8$). This suggests that at least an additional fourth relaxation mode does exist, although it is centered out of the experimental frequency window. To estimate the fourth relaxation time, the Debye model of the process is assumed. For this case the relaxation time can simply be calculated from the formula:

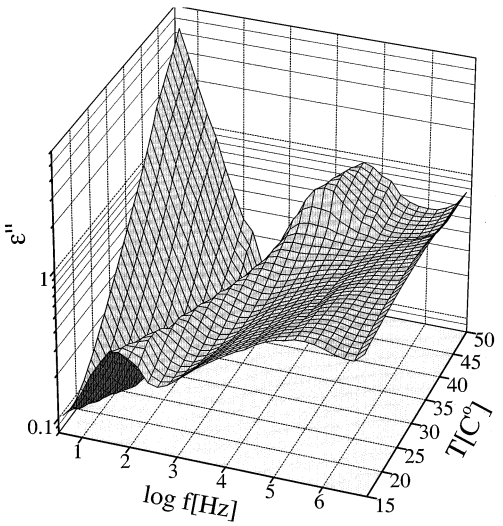

Figure 5. 3-D plot of dielectric loss ϵ'' for **3A** dendrimer as a function of frequency and temperature.

$$\tau = \frac{\epsilon''}{(\epsilon' - \epsilon_\infty)\omega} \quad (8)$$

The peak frequency of the fourth mode has been estimated to be about $f_4 = 10^8$ Hz (at 300 K) and is found to be only weakly affected by the orientational order. Relaxation spectra of ϵ' and ϵ'', in the measuring frequency range $1-10^7$ Hz, have been subsequently fitted for the three peaks using eq 6 for those processes. Parts a and b of Figure 7 show the plots of the dielectric strength and the relaxation frequency, respectively, for the three separate processes as a function of temperature. In the isotropic phase only two processes are seen. The low-frequency process is contributed by the longitudinal component, and the higher frequency component is contributed by the transversal component of the dipole moment. On approaching the I−N phase transition, the low-frequency mode diverges into processes f_1 and f_2. The temperature dependence of these modes clearly demonstrates that these are strongly affected by the orientational order. The third process, of the higher frequency, f_3, is considered to be the rotation of the perpendicular component of the dipole moment around the long molecular axis. Similarly, the fourth process, f_4, can also be related to the rotation around the long molecular axis. However, relatively high frequency of this mode suggests that only mesogenic core (or even only the biphenyl part with the carboxyl group and the terminal chain $OC_{11}H_{23}$) can contribute to this motion. Peak frequencies, the dielectric strength of each mode, and the low-frequency value of the permittivity ($\Delta\epsilon_\perp - \epsilon_{\infty\perp}$) are shown in Figure 7a,b. The dielectric strength

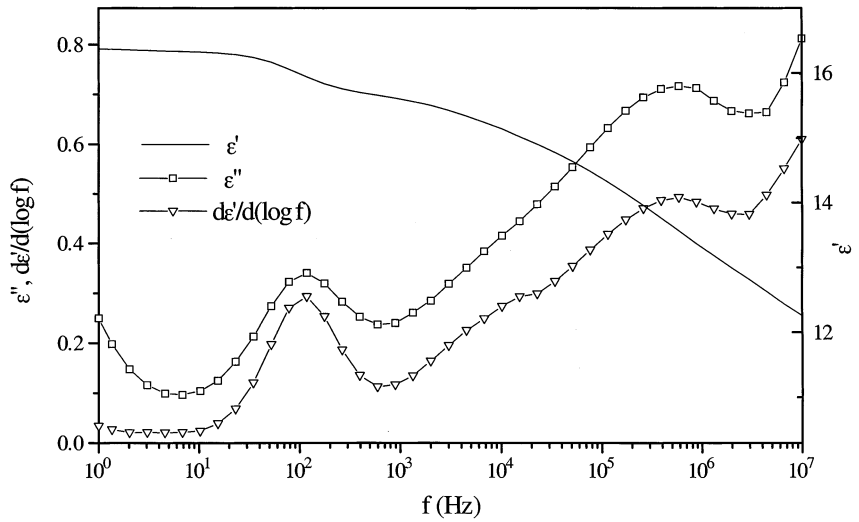

Figure 6. Frequency dependencies of the dielectric permittivity (real part ϵ', ▽; imaginary part ϵ'', □) and the derivative of ϵ' with respect to (log f) − ▽ for **3A** at a temperature of 298 K.

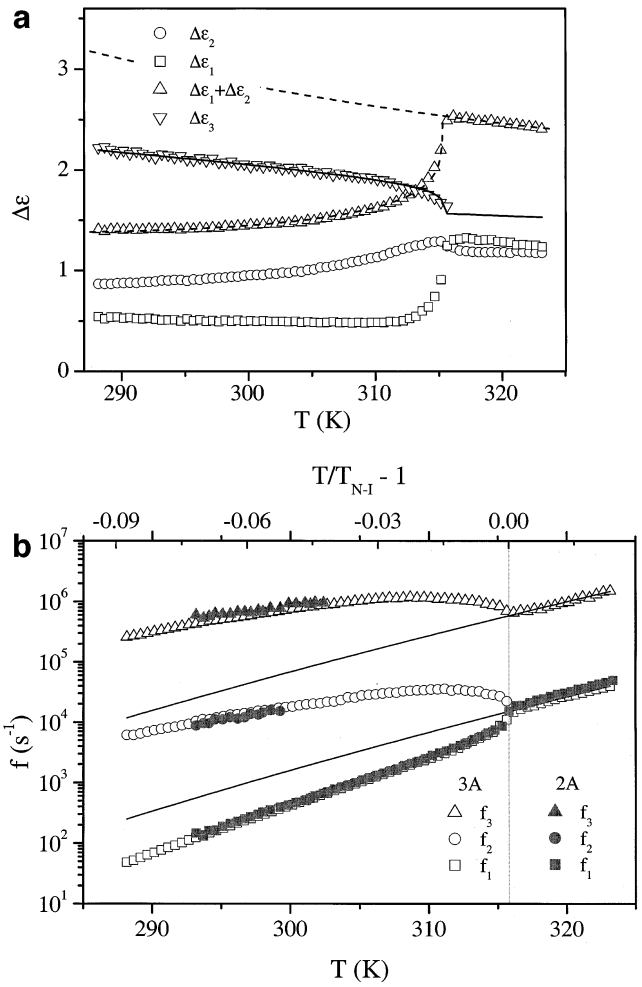

Figure 7. (a) Dielectric strength $\Delta\epsilon$ of the deconvoluted modes for **3A**: □, $\Delta\epsilon_1$; ○, $\Delta\epsilon_2$; ▽, $\Delta\epsilon_3$; △, $\Delta\epsilon_1 + \Delta\epsilon_2$ as a function of temperature in K The solid lines show the fitting of the M−M model to the experimental data. (b) Temperature dependencies of the relaxation frequencies of the three modes: □, f_1; ○, f_2; ▽, f_3, for compounds **2A** (open) and **3A** (solid). Data for **2A** are plotted on the reduced temperature scale.

of the fourth mode is calculated by subtracting contribution of each mode ($\Delta\epsilon_1$, $\Delta\epsilon_2$, and $\Delta\epsilon_3$) from $\Delta\epsilon_\perp = \epsilon_\perp - \epsilon_{\infty\perp}$.

Compound **2A** also shows very similar dielectric spectra with three peaks in the frequency window, and the evidence of the contribution of the highest frequency mode, f_4, in the $\Delta\epsilon_\perp$ component of the dielectric permittivity is also seen. For this compound, the corresponding peaks positions are shifted to the higher frequencies with respect to those observed for the **3A** dendrimer. Therefore, the spectral decomposition into peaks is possible only in the limited range of temperatures. It is convenient, however, to compare the peak frequencies of samples **2A** and **3A** in the reduced temperature scale also given in Figure 7b. The results for **2A** surprisingly overlap the data for **3A**. All the three modes (1, 2, 3), observed in the experimental frequency window, cannot be assigned to the rotation of the entire molecule but can only be assigned to the rotation of each arm of the dendrimer separately. The spacers of dendrimer are large and flexible enough so that the reorientation of the monomer part is decoupled from the reorientation of the central core. Therefore, we conclude that differences in the peak frequencies of the corresponding processes are only due to the lower viscosity of the compound **2A** in comparison to that of **3A**. Interestingly, the value of the normalized izotropization entropy ($\Delta S/Rn^{-1}$), which is related to the nematic ordering at the isotropization temperature, is almost independent of the size of the molecule whether it is a low molar mass material or a dendritic polymer.[8]

According to the Maier−Meier theory for the nematic phase, the contributions of the first and the second modes $\Delta\epsilon_1$ and $\Delta\epsilon_2$ are proportional to square of the longitudinal component of the dipole moment μ_l^2 and should follow formula 7b. So we can assign

$$\Delta\epsilon_l = \Delta\epsilon_1 + \Delta\epsilon_2 = \frac{NhF^2 g_l^{\perp} \mu_1^{\,2}}{3\epsilon_0 k_B T}(1 - S) \qquad (9)$$

The temperature dependence of the order parameter for the optically uniaxial phase is well described by mean-field theory[14] expressed in terms of eq 4, where b is critical power law exponent. The fitting of the experimental data to eq 9 with S described by eq 4 is shown by the solid line in Figure 7a. As a result of the fitting, we obtained $b = 0.235$ and $\mu_l = 0.81$ D. The critical exponent from the dielectric measurements is found to

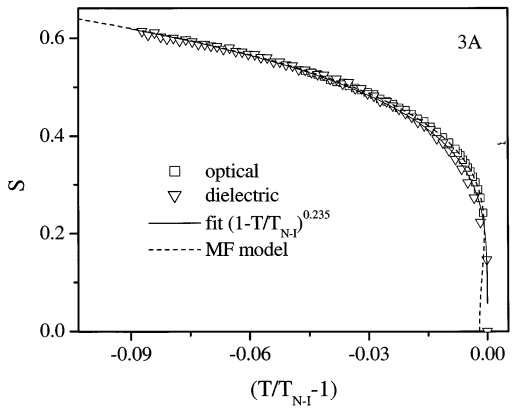

Figure 8. Orientational order parameters for **3A** dendrimeras a function of reduced temperature. Comparison of the results from birefringence (□), dielectric data (▽), and the fitting of the MF model (- - -).

be of similar value to that obtained from the optical method.

The third process is assigned to the rotation of the transverse component of the dipole moment around the long molecular axis using the relevant part of eq 7b. The dielectric strength of the mode can be fitted to the equation

$$\Delta\epsilon_3 = \frac{NhF^2 g_1^{\perp} \mu_t^2}{3\epsilon_0 k_B T}(1 + 0.5S) \qquad (10)$$

To reproduce $\Delta\epsilon_3$ from the Maier−Meier theory, the dependence of S on T is obtained from the low-frequency modes (Figure 7a). This allows the adjustment in the value of the transverse dipole component μ_t. The total transverse dipole moment, for the third and fourth modes, is found to be $\mu_t = 2.2$ D.

The dipole moments that contribute to the dielectric permittivity are located in the mesogenic core of the molecule, and these are the carboxyl group dipole and three dipoles of the alkoxy group. Obviously, the magnitude of the total dipole moment depends on the conformation of the dendrimer branches themselves. For the most probable extended conformation of the monomer part it is relevant to assume that alkoxy dipoles in terminal chains can compensate each other, so that the net contribution to the dipole moment arises from the combination of the dipoles of carboxyl and alkoxy groups in the ortho position of the benzene ring. Indeed, the effective value of the dipole moment is found from the dielectric strength as $\mu = 2.34$ D, where $\mu = (\mu_l^2 + \mu_t^2)^{1/2}$. The value of μ is a reasonable value for the net dipole moment estimated from the structure of the monomer. Molecular simulations can be carried out to arrive at a similar value. The angle θ between the dipole moment and the long molecular axis of the monomer is calculated to be $\theta \cong 70°$. It is important to note that the order parameter for **3A** obtained using both the dielectric and optical techniques agrees with each other within the experimental accuracy of the measurements. The order parameter is fitted to eq 5b (see the dashed lines in Figure 8), and the parameters of the best fit are listed in section 3.

3.4. Dynamics of the Molecular Relaxation Process. To analyze the low-frequency molecular process, it is convenient to use the Arrhenius equation $\tau = Ae^{E_a/kT}$, where A is the prefactor, E_a is the activation energy, and kT is the thermal energy at temperature T in kelvin. Taking the isotropic frequency f_0 as the reference, we found that the low-frequency process (f_1) is retarded and the middle frequency process (f_2) is accelerated. In a similar way, the frequency of the third mode can be fitted to the Arrhenius equation and extrapolated to the nematic phase. In the case of the latter, the rotation is accelerated compared to that extrapolated from the dependence in the isotropic phase. The frequency of the fourth mode shows its acceleration, but this does not seem so strongly affected by the orientational order.

The effect of the acceleration and the retardation of the processes can simply be analyzed in terms of the activation energy. In the nematic phase for the case of the end-over-end rotation, an additional contribution to the activation energy arises from the nematic potential. The theoretical prediction of the relaxation frequency in the nematic phase was obtained by Meier and Saupe[18] for the rigid molecules from the solution of the anisotropic diffusion equation. It was found that a single frequency is sufficient to describe the relaxation of a dipole moment component, and this can be expressed in terms of relaxation rate (f_0) for the particular dipole component in the absence of a nematic potential by

$$f_i = \frac{f_0}{j_i} \qquad (11)$$

The subscript i identifies the component of the permittivity, and the quantity j_i is a retardation (or acceleration) factor calculated numerically from the model. The parameter j_i depends on the parameter b of the nematic pseudopotential $u = -bS\cos^2\theta$, where θ is the angle between the long axis of a uniaxial molecule and the director. An approximate result for the retardation factor was calculated[18] such that

$$j_1 = \frac{k_B T}{bS}\left[\exp\left(\frac{bS}{k_B T}\right) - 1\right] \qquad (12)$$

where bS is identified as the height of the potential barrier for the end-over-end rotation of the molecule.

In general, the relaxation time depends on the parameters of the assumed pseudopotential and the anisotropy of the rotational diffusion constants $D_{\parallel}$ and $D_{\perp}$, which arise from the molecular shape and the local viscosity. The effect of the liquid crystal ordering potential is to decrease the relaxation frequency for the end-over-end rotation and to increase it for the rotation about the long molecular axis. If anisotropy of the rotational diffusion constants is included, then the relaxation time for the end-over-end rotation is further retarded, and in the same way rotation about the long molecular axis is further accelerated.

Retardation factors found for the tripole **3A** are shown in Figure 9. Results are quite different than found for the low molar mass nematogens. For conventional nematics, the acceleration for the rotation along the long molecular axis is rather weak, and the acceleration factor is found usually close to unity. For dendrimers, the acceleration effect is even stronger than the retardation for the end-over-end rotation. This suggests rather strong influence of the molecular shape and of the anisotropy of the rotational diffusion constants on the reorientation in the nematic phase.

The problem of the structural changes (mainly of the molecular shape) in the polymer has been studied by

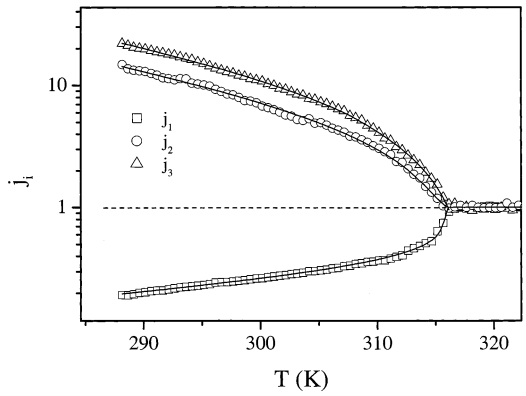

Figure 9. Retardation and acceleration factors for the **3A** dendrimer: □, j_1; ○, j_2; ▽, j_3 as a function of temperature in K.

Pickett and Schweizer[19] for the nematic phase in particular. On assuming that the chains interact only through the monomer−monomer excluded-volume interaction, the existence of the two density correlation lengths in the an-isotropic phase is demonstrated. Increasing the order parameter shrinks the invaded space of each chain, so that the neighboring chains overlap to lesser extent. The two density screening lengths, parallel $\xi_{||}$ and perpendicular $\xi_{\perp}$ to the director,[19] are given by

$$\xi_{\perp} = \xi\sqrt{1 - S}, \quad \xi_{\perp} = \xi\sqrt{1 + 2S} \tag{13}$$

where ξ is the screening length in the isotropic phase. As a consequence of such anisotropy and because the monomer is adapting more calamitic shape, the rotation around the long molecular axis is expected to undergo much smaller friction in the nematic than in the isotropic phase. Following the molecular theory for rotational diffusion tensor,[17,20] and using the experimental value of the retardation factors, the ratio $D_{||}/D_{\perp}$ has been found to increase by a factor of 20 in the nematic phase at $T = 298$ K compared to the value at the nematic−isotropic phase transition temperature. On the other hand, this ratio $D_{||}/D_{\perp}$ can be estimated from the molecular shape. The dependence of the molecular shape on the rotational diffusion coefficients was studied using the hydrodynamic model[21,22] in terms of the anisotropy of the molecular friction for the slip boundary conditions. The ratios of the basic dimensions for the monomer shape were assumed to be $a/c = 0.2$ and $b/c = 0.3$ (where a, b, and c are the basic dimensions along the x, y, and z axis of the monomer, respectively), and they were used as inputs to the hydrodynamic model. The ratio $D_{||}/D_{\perp} \cong 23$ found from the model is in good agreement with the experimentally determined value with the accuracy limited by the molecular shape evaluation.

4. Conclusions

The orientational order parameters have been determined from the birefringence and refractive indices for **2A** and **3A** multipodes in the nematic phase. The critical exponents are found to be very close to that for the so-called "three-critical behavior". A detailed analysis of S found that the I−N phase transition is weakly first order. The order parameter, determined from dielectric spectroscopy, is in good agreement with that found from the optical technique.

At least three molecular modes were resolved in the dielectric relaxation spectra of the multipodes **2A** and **3A** in the nematic phase. These are the end-over-end rotation, the processional motion about the director, and the rotation about its own long molecular axis, called the spinning motion. The first process is retarded, and the other two are accelerated with respect to their relaxation rate in the isotropic phase. The acceleration factors are found to be much greater than for the conventional nematic liquid crystals. This behavior is quantitatively analyzed in terms of the nematic potential and the anisotropy of the molecular shape.

The dielectric spectra, optical birefringence, and the refractive indices are mostly controlled by the orientational order and the properties of the monomer. The results are interpreted in terms of the mesogen being decoupled from the size of the dendrimers. The comparison of the acceleration and deceleration factors for the dendrimers with the low molar mass nemotegens indicates that anisotropy of the molecular shape plays an important role in controlling the nematic potential.

Acknowledgment. Research work was funded by the EU network on Liquid Crystalline dendrimers HPRN-CT-2000-0016. A. Kocot thanks the Committee for the Scientific Research (KBN) for Grant 2P03B 09817, and J.K.V. thanks the Enterprise Ireland for grant under the international collaboration fund. We thank Dr. Olga Kalinovskaya for her help and for discussions.

References and Notes

(1) (a) Baars, M. W. P. L.; Söntjens, S. H. M.; Fischer, H. M.; Peerlings, H. W. J.; Meijer, E. W. *Chem. Eur. J.* **1998**, *4*, 2456. (b) Lorenz, K.; Hölter, D.; Stühn, B.; Mühlhaupt, R.; Frey, H. *Adv. Mater.* **1996**, *8*, 414. (c) Ponomarenko, S. A.; Rebrov, E. A.; Bobrovsky, A. Y.; Boiko, N. I.; Muzafarov, A. M.; Shibaev, V. P. *Liq. Cryst.* **1996**, *21*, 1.

(2) (a) Richardson, R. M.; Ponomarenko, S. A.; Boiko, N. I.; Shibaev, V. P. *Liq. Cryst.* **1999**, *26*, 1. (b) Percec, V.; Chu, P. W.; Kawasumi, M. *Macromolecules* **1994**, *27*, 4441. (c) Cameron, J. H.; Facher, A.; Lattermann, G.; Diele, S. *Adv. Mater.* **1997**, *9*, 398.

(3) (a) Ibn-Elhaj, M.; Coles, H. J.; Guillon, D.; Skoulios, A. *J. Phys. II* **1993**, *3*, 1807. (b) Date, R. W.; Imrie, C. T.; Luckhurst, G. R.; Seddon, J. M. *Liq. Cryst.* **1992**, *12*, 203. (c) Li, M.-H.; Detre, L.; Cluzeau, P.; Isaert, N.; Nguyen, H. T. *Liq. Cryst.* **1998**, *24*, 347.

(4) Tschierske, C. *J. Mater. Chem.* **1998**, *8*, 1485. (b) Mehl, G. H.; Goodby, J. W. *Chem. Ber.* **1996**, *129*, 521. (c) Mehl, G. H.; Goodby, J. W. *Chem. Commun.* **1999**, *13*. (d) Percec, V.; Turkaly, P J.; Asandai, A. D. *Macromolecules* **1997**, *30*, 943.

(5) (a) Hessel, P.; Finkelmann, H. *Polym. Bull. (Berlin)* **1985**, *14*, 3751. (b) Gray, G. W.; Hill, J. S.; Lacey, D. *Mol. Cryst. Liq. Cryst.* **1991**, *197*, 43. (c) Lecommandoux, S.; Achard, M. F.; Hardouin, F. *Liq. Cryst.* **1998**, *25*, 85. (d) Sunder, A.; Quincy, M.-F.; Mühlhaupt, R.; Frey, H. *Angew. Chem., Int. Ed.* **1999**, *111*, 3107; *Angew. Chem.* **1999**, *38*, 2928.

(6) Veith, M.; Elsässer, R.; Krüger, R.-P. *Organometallics* **1999**, *18*, 656.

(7) Elsässer, R.; Mehl, G. H.; Goodby, J. W.; Photinos, D. J. *Chem. Commun.* **2000**, 851.

(8) Elsässer, R.; Mehl, G. H.; Goodby, J. W.; Veith, M. *Angew. Chem., Int. Ed.* **2001**, *40*, 2688.

(9) Dunmur, D.; Toriyama, K. In *Handbook of Liquid Crystals;* Demus, D., Goodby, J. W., Gray, G. W., Spiess, H. W., Vill, V., Eds.; Wiley-VCH: New York, Vol. 1, Chapter VII.

(10) Neugebauer, H. E. J. *Can. J. Phys.* **1950**, *28*, 292. Neugebauer, H. E. J. *Can. J. Phys.* **1954**, *32*, 1.

(11) Vuks, M. F. *Opt. Spectrosc.* **1966**, *20*, 361.

(12) Barbero, D.; Malvano, R.; Omini, M. *Mol. Cryst. Liq. Cryst.* **1977**, *39*, 69.

(13) Desai, R.; Pratap, R. *Mol. Cryst. Liq. Cryst.* **1981**, *75*, 287.

(14) deGennes, P. G.; Prost, J. *The Physics of Liquid Crystals*; Oxford University Press: Oxford, UK, 1993.

(15) Havriliak, S., Jr.; Negami, S. *J. Polym. Sci., Part C: Polym. Symp.* **1966**, *14*, 99.

(16) Maier, W.; Meier, G. Z. *Naturforsch.* **1961**, *16a*, 262.

(17) Haws, C. M.; Clark, M. G.; Attard, G. S. Dielectric Relaxation Spectroscopy of Liquid Crystals. In *Side Chain Liquid Crystal Polymers*; McArdle, C. B., Ed.; Blackie: Glasgow, 1989; p 196.
(18) Meier, G.; Saupe, A. *Mol. Cryst. Liq. Cryst.* **1966**, *1*, 515.
(19) Pickett, G. T.; Schweizer, K. S. *J. Chem. Phys.* **2000**, *112*, 4869.
(20) Nordio, P. L.; Rigatti, G.; Segre, U. *Mol. Phys.* **1973**, *25*, 129.
(21) Hu, C.; Zwanzig, R. *J. Chem. Phys.* **1974**, *60*, 4353.
(22) Youngren, G. K.; Acrivos, A. *J. Flud Mech.* **1975**, *69*, 377. Youngren, G. K.; Acrivos, A. *J. Chem. Phys.* **1975**, *63*, 3846.

MA020714P